

The role of salt in nanoparticle generation by salt-assisted aerosol method: Microstructural changes

Seung Geun Lee, Sung Min Choi, Donggeun Lee*

*School of Mechanical Engineering, RIMT, Pusan National University, Janggeun-dong, Geumjeong-gu,
Busan 609-735, Republic of Korea*

Available online 1 December 2006

Abstract

We described the possible roles of an inert salt such as NaCl in spray pyrolysis and aerosol–gel syntheses of nanoparticles. We demonstrated that the salt acts primarily as a filler to inhibit further agglomeration of preexisting SiO₂ sols as well as co-precipitated CuO particles. Depending on the contents of the salt, we observed that the microstructures of nanoparticles range from nano dots to mesoporous particles. During the aerosol–gel reaction, in particular, the salt could accelerate the reaction faster. Possible mechanisms will be discussed in detail.

© 2006 Elsevier B.V. All rights reserved.

Keywords: Inert salt; Microstructure; Nanoparticle; Dots; Fragments; Mesoporous

1. Introduction

Since ultrafine particles display highly desirable traits such as enhanced catalytic performance, lowered sintering temperature, higher density [1,2], and higher energy release [3] due to enhanced reactivity [4,5], the particles are currently of great interest for a wide variety of applications, ranging from electronics through ceramics to catalysts. As the changes in such properties are originated from the so-called ‘quantum size effect’, many researchers have devoted to develop efficient methods to generate smaller and smaller particles. The methods reported from literatures can be mainly classified into liquid-, vapor-phase, and more recent aerosol-based synthesis.

Sol–gel synthesis [6], the most popular liquid-phase method, has been widely used for generation of various metal oxide nanoparticles. Though the particles are typically very small as the sol–gel reaction can occur even at room temperature, they are strongly aggregated, which has been acknowledged nearly unavoidable without use of steric stabilization agents. Some surfactants are recently applied to inhibit the aggregation during a sol–gel synthesis of semiconductor nanoparticles, with a control of particle size [7]. But, since the method requires additional processes, for examples, calcination to remove the organic

surfactants, a microstructure of the as-received particles can be collapsed during the process.

The vapor-phase synthesis including flame and evaporation/condensation has been employed in particular for large-scale production due to its easy scale-up and continuous production. Though the time for the production is typically much shorter than that of the liquid-phase method, it is not easy to control the size and morphology of particles [1,2]. Aerosol-based method such as aerosol–gel [3,8,9] or spray pyrolytic synthesis [5,10–13] seems to take each unique benefit of the liquid- and vapor-phase methods. In fact, the aerosol method cannot only confine the reaction or aggregation zone within a droplet but also evaporate the solvent within a few second [14]. Moreover, this method can produce various, for examples, metal [11], metal oxide [9–14], and semiconductor nanoparticles [15].

Together with the efforts for reducing the particle size, some people has devoted to control the morphology of particles by altering systematic parameters or adding an inert agent like salt to the precursor [9,12,13]. Depending on the experimental conditions used for the aerosol-based synthesis, the particles have very different morphologies from shell-like via dense-solid to porous structures. While Okuyama group [12,16] showed that the addition of inert salt to a precursor solution and subsequent water-rinsing led to the breakup of sub-micrometer particles into much smaller particles (<20 nm), Zachariah and co-workers demonstrated that the salt addition increases porosity of particles generated from aerosol–gel [9] and spray pyrolysis [13] synthesis, with no change in overall particle size.

* Corresponding author. Tel.: +82 51 510 2365; fax: +82 51 512 5236.
E-mail address: donglee@pusan.ac.kr (D. Lee).

Regarding the simplicity of the method and economical reuse of the salt, it is surprising to find that there are no more relevant researches to describe this discrepancy between the two reports. Therefore, we describe in this work two experiments which are designed to better understanding the roles of the salt in either of the aerosol–gel synthesis of mesoporous SiO₂ particles and the spray pyrolysis synthesis of CuO particles. We investigate the effects of systematic parameters such as reaction temperature, relative concentration of the salt to a precursor, on the size, morphology, and crystallinity of particles.

2. Experimental

2.1. Salt-assisted spray pyrolysis of CuO nanoparticles

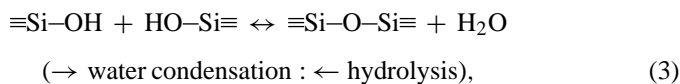
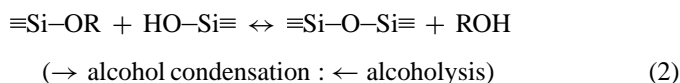
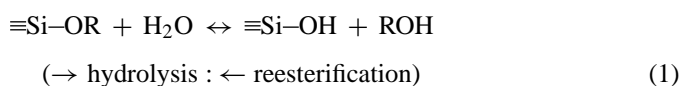
Fig. 1 shows the experimental setup for generating nanoparticles using spray pyrolysis which is essentially similar to that used for our previous spray pyrolytic synthesis of metal oxide [5]. A solution of copper nitrate is prepared by mixing commercially available copper nitrate (>99% in purity) with filtered deionized (DI) water which was then atomized in air to generated aerosol droplets of the solution. The concentration of the nitrate is kept constant with 0.05 mol dm⁻³ unless otherwise stated. At this step, different amounts of NaCl is added into the solution, leading to the changes in the molar mixing ratio of NaCl/Cu(NO₃)₂ from 0 to 1.5.

The droplet-laden air is then passed through a diffusion dryer filled with dry silica gel to remove most of water content in the droplets, and delivered to a heated flow tube. The heated flow tube is made of stainless steel with 1.0 cm i.d. and 40 cm long, and is suspended in a 3 cm i.d. alumina tube placed in a tube furnace with a heated length of 30 cm. This arrangement eliminates hot spot in the stainless steel tube, which could be caused by uneven furnace heating elements or by contact between the alumina and the stainless steel tube. A third of the aerosol flow (~3 lpm) from the atomizer is delivered to the heated tube by detouring the excess flow, in order for the droplets to get sufficient time for decomposition. The residence time of the droplet in the hot zone is about 2 s. The temperatures of the furnace are varied from 425 to 700 °C to see a temperature effect. Except for this case, the temperature is maintained constant with 600 °C that is high enough for complete decomposition of copper nitrate. As such, the particles generated are collected on a filter and the NaCl existing in the particle is then washed by DI water as seen in Fig. 1.

2.2. Salt-assisted aerosol–gel synthesis of SiO₂ particles

The term of “aerosol–gel” means a method combining a conventional sol–gel reaction with an aerosol processing. The aerosol processing including the pre-mentioned spray pyrolysis has a number of advantages over the batch processing in a beaker. To apply the aerosol processing to the batch processing, we can only mist the precursor solution or partially reacted sol–solvent mixture in the beaker. The experimental setup of the apparatus used for the aerosol–gel synthesis is therefore exactly same as that described in the previous section.

The precursor solution is prepared by dissolving tetraethoxysilane (TEOS, Si[O(CH₂CH₃)₄]) in the mixture of HCl, DI water, and ethanol (EtOH). The basic sol–gel chemistry for silica formation [6] from silicon-alkoxide precursor is as follows.



where R is an alkyl group, C_xH_{2x+1}. The hydrolysis in Eq. (1) is most rapid and complete when catalysts are employed. Since rapid hydrolysis produces a lot of Si–OH, the preferred water condensation (Eq. (3)) likely dominates dimerization process as a first step for gelation.

Decreasing the size of silica sols (primaries composing an silica aggregate) is most important and a fundamental requirement for the production of ultrafine isolated or mesoporous particles. Under the acidic condition of pH 2–7, the sol–gel reaction very often produces fine sols with a few nanometers in size. Such a acidic condition would therefore be chosen rather than a basic condition where significant growth of the primaries occurs due to Ostwald ripening [6]. In addition, as point of zero charge (PZC) of silica particles in water is about 2, the added acid destabilizes the colloidal sols in the water leading to fast gelation or aggregation between sols [17], which is needed to enhance production rate. In this respect, we select mineral acid

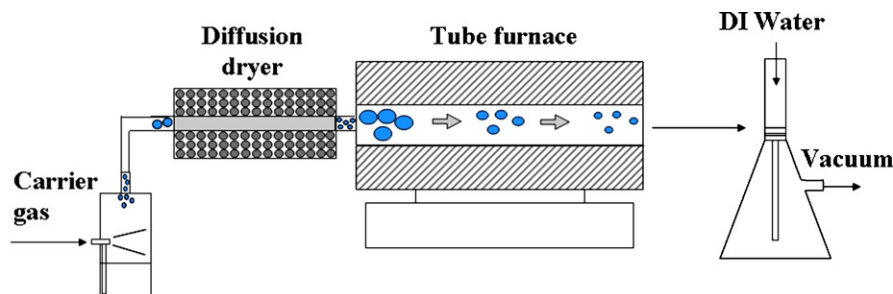


Fig. 1. Schematic of a salt-assisted aerosol-based synthesis of nanoparticles via sol–gel reaction and spray pyrolysis.

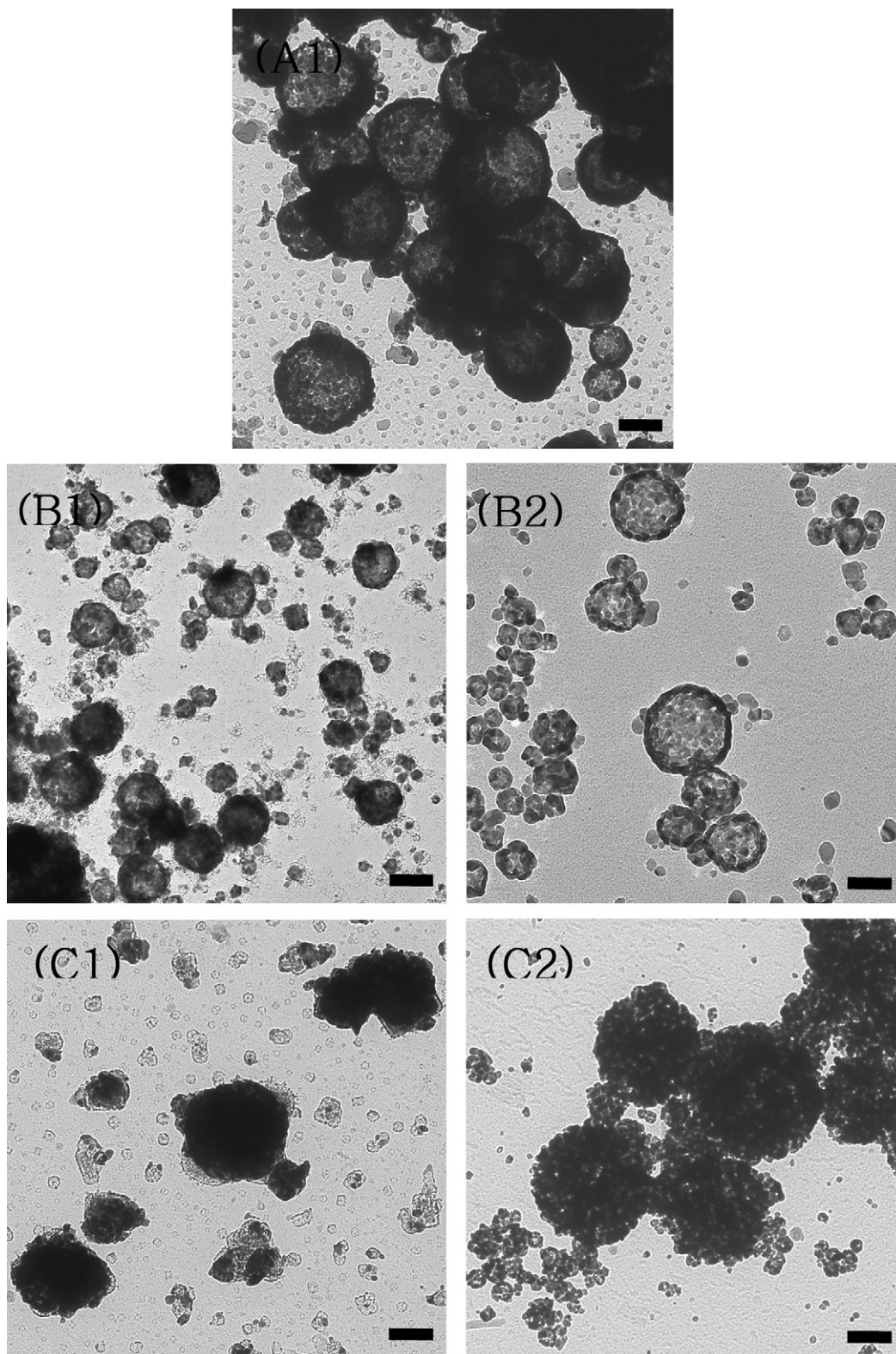


Fig. 2. Morphology changes of CuO particles with increasing NaCl content. The left-side and right-side photos represent TEM images before and after washing. (A–D) correspond to the particles at various mole ratios of $\text{Cu}(\text{NO}_3)_2:\text{NaCl}$ of 1:0, 1:0.3, 1:0.75, and 1:1.5, respectively. The temperature for spray pyrolysis reaction is kept constant at 600 °C. The bar represents 100 nm in size.

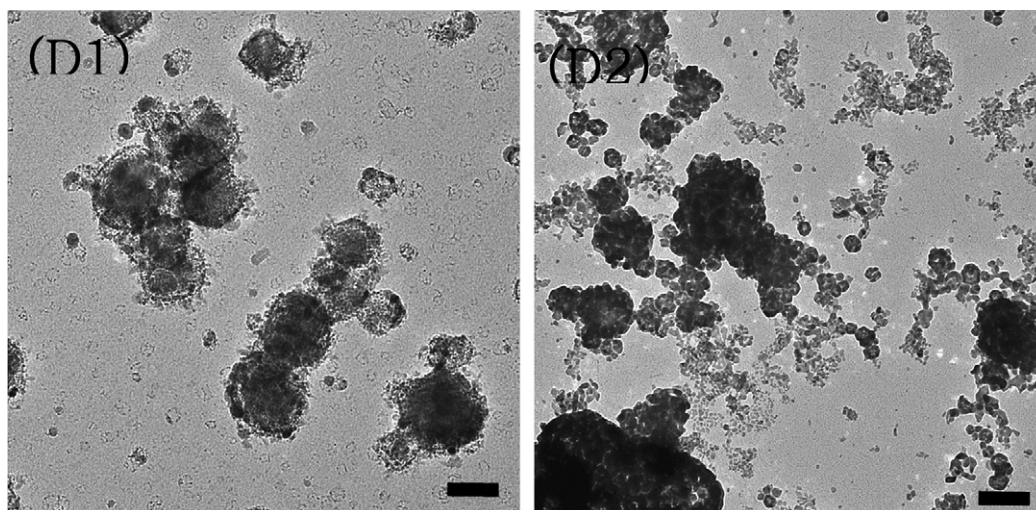


Fig. 2. (Continued).

(HCl), one of the most general catalysts in the sol–gel processing to keep the pH of the precursor solution at around 3. The mixing molar ratio of TEOS/EtOH/H₂O/HCl is 1:58:251:0.7. Four-times larger amount of the NaCl than the TEOS is then added into the solution maintaining at 60 °C as well as being stirred. Note that the NaCl is readily dissolved in the excess water with no precipitation. All chemicals obtained from Aldrich Co. are used with no more purification.

We define the time elapsed from the addition of the NaCl to the atomization of the solution as the gelation time (t_g). As the t_g is going, the three-dimensional networking between sols gets more strengthen in the beaker. Once a part of the solution at a selected time is aerosolized (misted) to micron-sized droplets, the solvent is evaporated very shortly in the flow tube heated at 150 °C. If the characteristic time for the evaporation is so short, the NaCl is re-solidified to frozen the initial structure before further gelation takes place. Thus, by changing the t_g , we may be able to produce composite particles with the structures of silica networks or isolated sols supported by the NaCl. Subsequent washing the NaCl out of the particles seems to reveal the initial silica structure that ranges from isolated to porous internal structure.

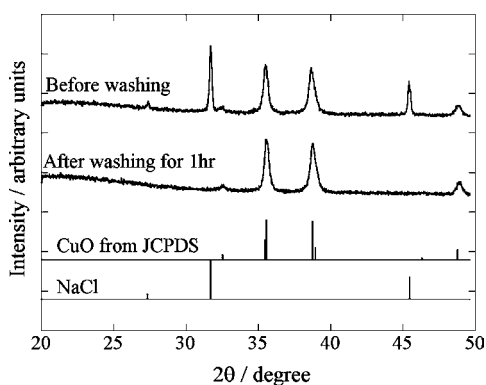


Fig. 3. X-ray diffraction patterns of CuO particles before and after washing the NaCl. The particles are spray-pyrolyzed at 600 °C and the mole ratio of Cu(NO₃)₂:NaCl = 1:0.75.

3. Results and discussion

3.1. Salt-assisted spray pyrolytic synthesis of CuO nanoparticles

3.1.1. Effects of a ratio of NaCl to copper nitrate on morphology

We alter the ratio of NaCl to Cu(NO₃)₂ within a range between 0 and 150 mol%, to see the effect on the morphology of the spray-pyrolyzed CuO particles. Left-hand-side images in Fig. 2 show that hollow structure (A1) of CuO particles with no inclusion of the NaCl are collapsed to solid-like denser structure (C1) as the ratio of the NaCl increases up to 75%. At relatively low content of the salt, it appears unlikely that the salt takes significant effects on particle growth and morphology. When the NaCl is added 150% larger than Cu(NO₃)₂, the solid structure seems to begin to be fragmented (see Fig. 2D1).

According to Lenggoro et al.'s model [14], if evaporation of solvent occurs faster than the diffusion of solute, one may

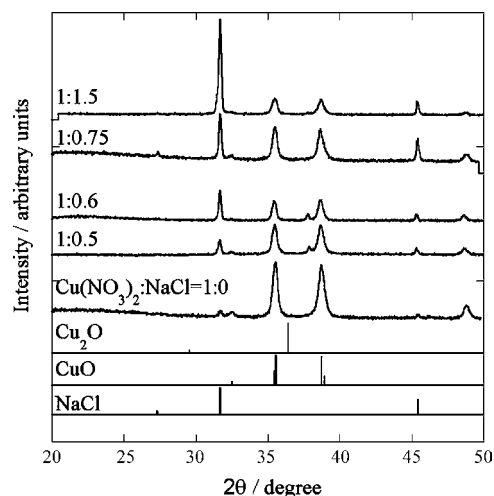


Fig. 4. XRD patterns of CuO particles generated at 600 °C with various NaCl contents.

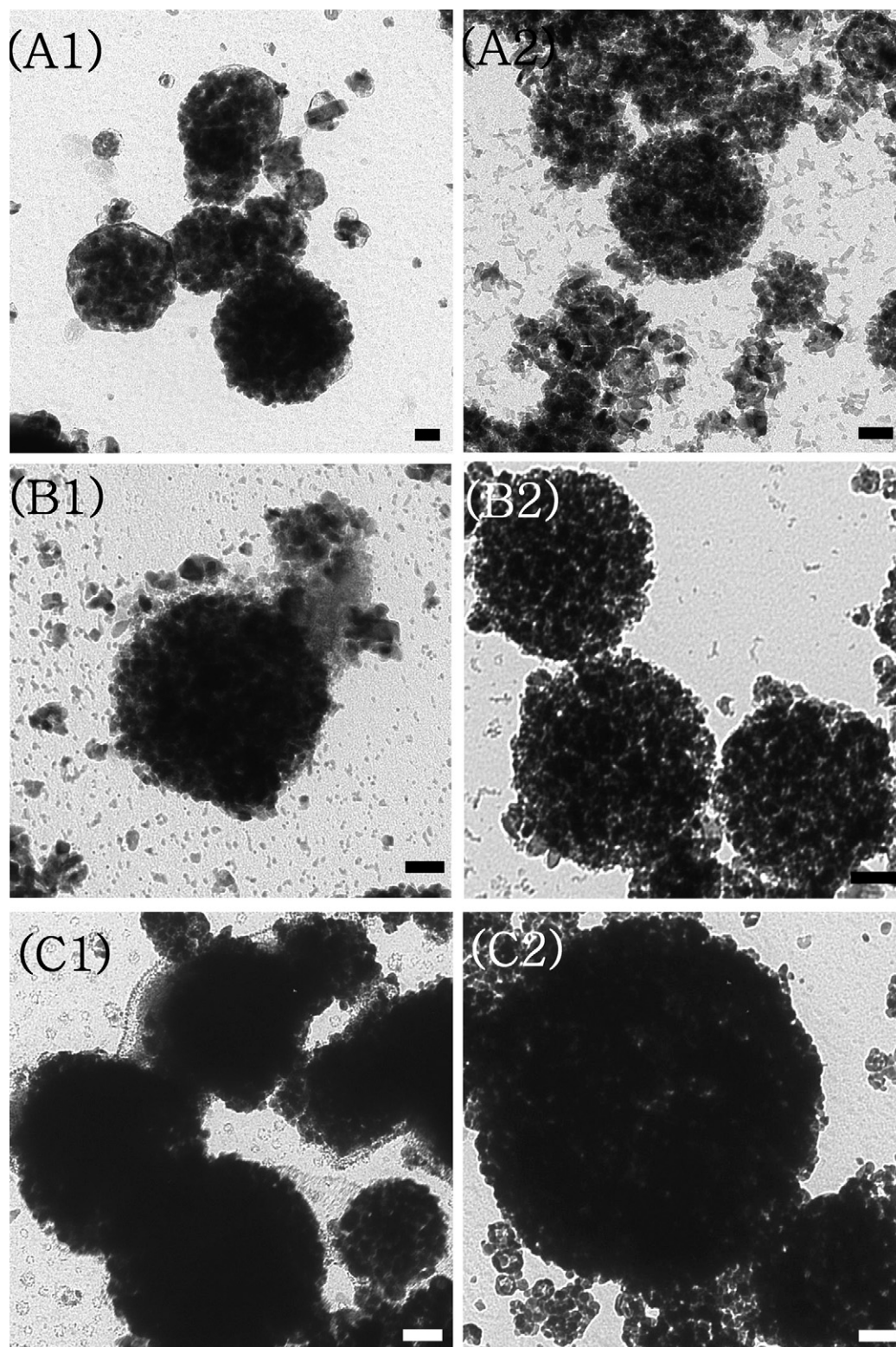


Fig. 5. The evolution of CuO–NaCl composite particles with increasing temperatures from (A) 425 °C through (B) 500 °C and (C) 600 to 700 °C, at constant mole ratio of $\text{Cu}(\text{NO}_3)_2\cdot\text{NaCl}=1:0.75$. The figures at the left and right column correspond to the TEM images of the particles before and after washing with water, respectively. The bar represents 100 nm.

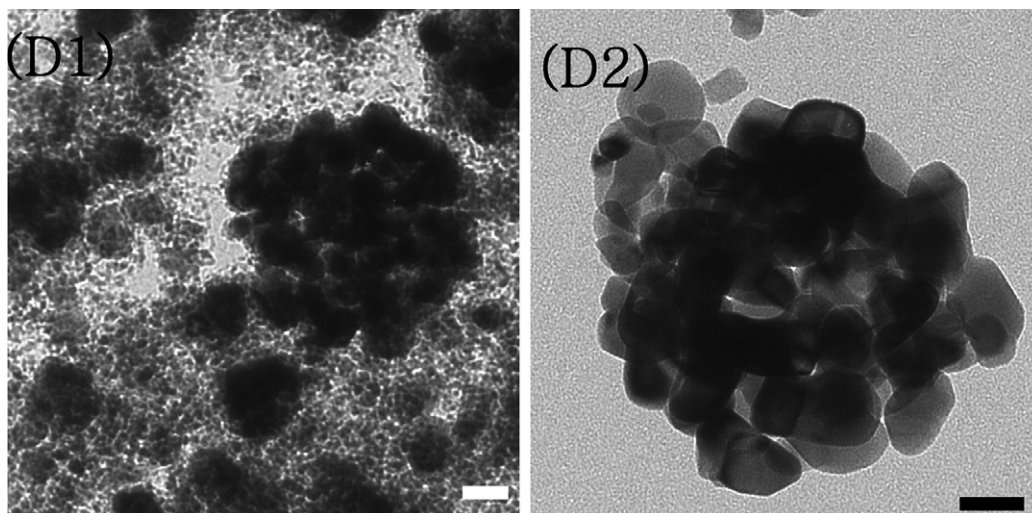


Fig. 5. (Continued).

expect faster increase of a precursor concentration near surface. When the highest concentration goes up more than a critical super-saturation concentration (CSC), the precursor begins to be re-solidified starting from the droplet surface, thereby leading to a crust formation. As the crust is thought hard enough to resist pyrolytic reduction in the volume, one may often observe hollow-structured particles during spray pyrolysis. Therefore, the TEM image seen in Fig. 2A1 may say that this experimental condition without addition of the NaCl corresponds to the faster evaporation. Regarding this, we may expect that higher precursor content tends to decrease the concentration gradient inside a droplet, forcing therefore the precipitation to occur in the whole region of a droplet. It is notable that higher dose of the NaCl to the precursor solution causes the increase of the total salt content. Thus, this can be at least one of the reasons for the morphology change with increasing the amount of the NaCl addition.

There is one more factor, that we should consider, i.e., solubility difference between the two salts, NaCl and $\text{Cu}(\text{NO}_3)_2$. Since copper nitrate has a higher solubility in water than that of the NaCl approximately by a factor of four (138 g/100 ml water for $\text{Cu}(\text{NO}_3)_2$; 36 g/100 ml water for NaCl), the NaCl would be first solidified during the drying process of the water. Whereas, the $\text{Cu}(\text{NO}_3)_2$ might remain in the dissolved state until the concentration of the nitrate reaches its CSC. In this respect, we may postulate that surface covering by the NaCl retards the evaporation of water, and such a solid-like structure is therefore preferred.

Here is the third explanation for the role of the NaCl. If the NaCl content is high enough to solidify either deeply to the center of the droplet from the surface or homogeneously throughout the particle, the precipitated NaCl nuclei are likely suspended and/or loosely contacted each other in 3D networks of CuO. Here, a removal of the NaCl by washing the particles results in the production of porous particles as confirmed in Fig. 2C2. Therefore, the salt acts as a filler to inhibit further coalescence between primaries in a CuO agglomerate.

Conversely, if too much NaCl is added, some of $\text{Cu}(\text{NO}_3)_2$ or partially pyrolyzed CuO can be isolated or very loosely contacted each other by a surrounding NaCl matrix. If this is the case, washing the NaCl yields partially fragmented structure (see Fig. 2D2). In this way, if one is interested in producing the mesoporous particles aiming at an application for catalyst, there exists an optimum ratio between the NaCl and $\text{Cu}(\text{NO}_3)_2$, near 75% (see Fig. 2C2). Therefore, we would say that the NaCl salt plays multiple roles in this spray pyrolysis synthesis, depending on the relative content of the NaCl.

As the fourth reason that might be attributed to the morphology change, one may raise the role of NaCl as an electrolyte destabilizing the CuO nuclei in water [17]. But, this requires for the NaCl to stay in the dissolved state even when the $\text{Cu}(\text{NO}_3)_2$ precipitates or is pyrolyzed. This is nearly impossible because the NaCl should be first precipitated due to its lower solubility than that of the $\text{Cu}(\text{NO}_3)_2$.

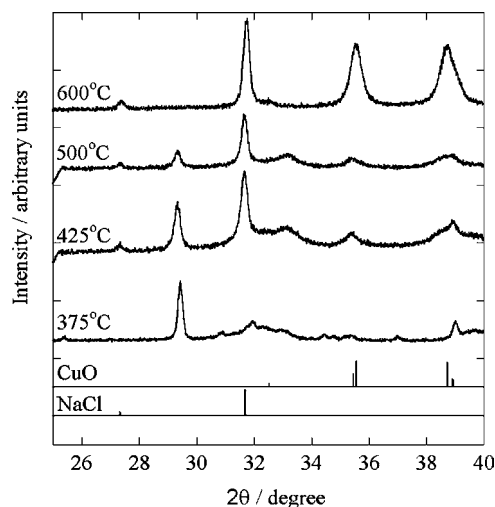


Fig. 6. XRD patterns of NaCl-containing CuO generated at different furnace temperatures.

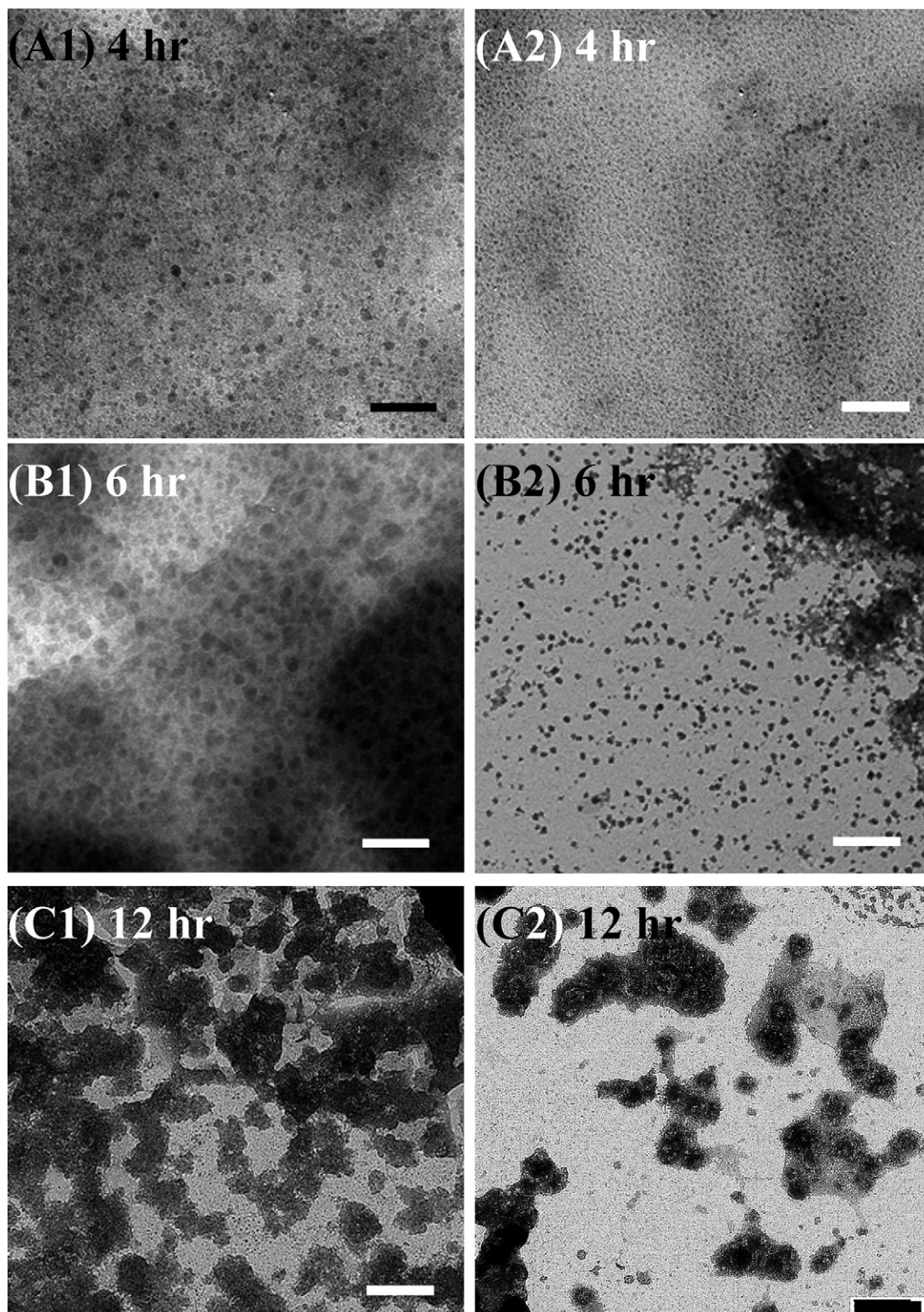


Fig. 7. (A–C) Evolution of silica particles in a beaker with increasing the gellation time t_g . The bar represents 200 nm. The right-hand-side images correspond to those of particles after washing.

3.1.2. Effect of the NaCl contents on the crystallinity of the CuO

Fig. 3 shows changes of X-ray diffraction (XRD) patterns of the CuO particles before and after washing the NaCl, together

with denoting peaks of CuO and NaCl from JCPDS database. Comparing the first two patterns from the above, the washing for more than 1 h is thought long enough for complete removal of the NaCl. Fig. 4 shows the XRD patterns of as-received CuO

particles generated with the various contents of the NaCl. The result shows that there is no distinct difference in the crystallinity of CuO particles as the NaCl is added more and more. Also, at this experimental condition, no relevant suboxide, Cu_2O , is observed. At the presence of H_2 , fast heating of CuO to a high temperature above 450°C results in a partial reduction of CuO to Cu_2O [18]. But, since our reacting system does not have such a reducing agent, the CuO appears as the only thermodynamically stable phase.

The width of the biggest peak of CuO in Fig. 4 remains nearly constant while the ratio of NaCl to $\text{Cu}(\text{NO}_3)_2$ increases to 75% from 0, but further addition of NaCl reveals a little bit more broaden peak. Accounting for this, we apply Scherrer formula for the peak width of CuO to estimate the crystallite size. The size of particles generated under less dose of the NaCl is about 18 nm, while for the 150% ratio, the size decreases to 13 nm. This is reasonably consistent with the observation by TEM, that the size of primary particles composing a big spherical cluster does not change much in spite of the big changes in the morphology (see Fig. 2A1, B2 and C2), whereas Fig. 2D2 shows the existence of smaller primaries.

3.1.3. Effect of reactor temperature on particle formation

In this section, the mole ratio of NaCl to $\text{Cu}(\text{NO}_3)_2$ is kept constant at 75%, the best composition for the production of the mesoporous particles. On the other hand, we change the heating temperature from 425 to 700°C to observe how the role of the salt is differed with the rising temperature. As the furnace temperature is rising up to 600°C , there is no remarkable change of either size or morphology, but one may notice a little structural densification (see in Fig. 6A–C). But, at 700°C close to the melting point of the NaCl ($\sim 800^\circ\text{C}$), we observe considerable growth of the primaries as well as the existence of very fine nuclei. Kim et al. [13] measured size distribution of Al_2O_3 –NaCl composite particles generated through similar routes. They found that a nucleation mode in the distribution began to appear at 700°C , which means the salt even below its melting temperature can evaporates in part and then nucleates. The fine nuclei in Fig. 5D1 is therefore a signature of the renucleation, implying that the NaCl is in a molten phase. In this case, the CuO agglomerates can be self-sintered with no

obstacle. That is why the CuO primaries grow significantly. The disappearance of such nuclei after washing supports again this inference.

The XRD patterns seen in Fig. 6 indicate the progress of spray pyrolysis reaction of the copper nitrate with temperature. It is notable that there is an unspecified peak around $2\theta = 29.5^\circ$, decreasing with increasing temperature. As the peak looks related to an unidentified intermediate product, the structural densification in Fig. 5A2–C2 may be related to the escape of NO_x gases and subsequent a little collapse of the structure.

3.2. Salt-assisted aerosol–gel synthesis of SiO_2 nanoparticles

3.2.1. Role of salt during the progress of the sol–gel reaction in a beaker

We need first to know the progress of the sol–gel reaction in a beaker prior to atomizing the solution. By changing the t_g for which the batch reaction occurs, we can change the initial state of the droplet that will be imposed to aerosol processing. To imaging the particles in the beaker at a selected time, we sample some of the particles by dipping a TEM grid to the diluted solution and then dry the grid rapidly at room temperature within ~ 10 min.

Fig. 7 indicates the evolution of SiO_2 particles in the presence of NaCl with the progress of the sol–gel reaction (increasing the t_g). Fig. 7A shows the hydrolysis/condensation in Eqs. (1)–(3) is not complete at the early gellation time (t_g) of 4 h. The gray background is revealed to comprise partially reacted precursor and precipitated NaCl (will be discussed later). The precipitation of the salt during the rapid drying helps to maintain the original structure in the beaker. After removal of the NaCl as seen in Fig. 7A2, the sol particles in Fig. 7A1 are left, but with a little size reduction. As the reaction is going further to 6 h, the particles are growing maintaining their shapes. After washing the salt, we obtain a clear image of isolated spherical sol particles (see Fig. 7B2). This reflects that the salt avoid the contacts between the sols. At $t_g = 12$ h, there is a remarkable change in the structure. The partially reacted background seems to be disappear, but the precipitated salt stay there. As the NaCl removal does not cause considerable structural changes, the rigid three-dimensional networks are formed between the particles, i.e., say the state of ‘gel’. The size distributions of the salt-removed silica particles are shown in Fig. 8. It should be emphasized that the 6 nm silica sols are stabilized by the co-precipitation of the inert salt and it is now possible to avoid the strong agglomeration, a weak point of a conventional sol–gel route as well.

We performed similar experiments for decreasing the NaCl content (TEOS:NaCl = 1:1 and 1:0). At the beginning of the apparent sol formation, the TEM images of the particles reveal the similar structure in Fig. 7A1 (not shown), but the time necessary for the reaction is significantly delayed with decreasing NaCl content. For example, 4 h at the ratio of 1:4 increases gradually up to 16 h in the absence of the salt. Therefore, in this sol–gel batch reaction, we may conclude that the salt apparently not only catalyzes the reaction but also inhibits the agglomeration especially at the early time. Moreover, the drying should

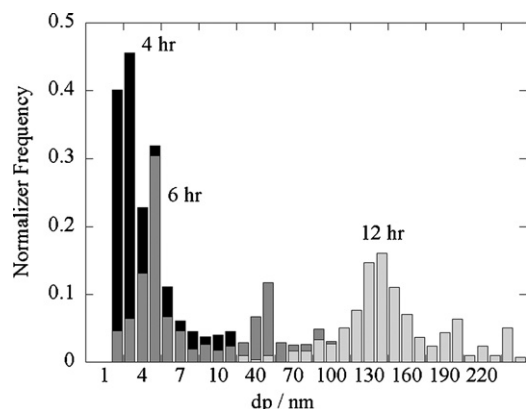


Fig. 8. The size distributions of primary particles seen in Fig. 7A2, B2, and C2.

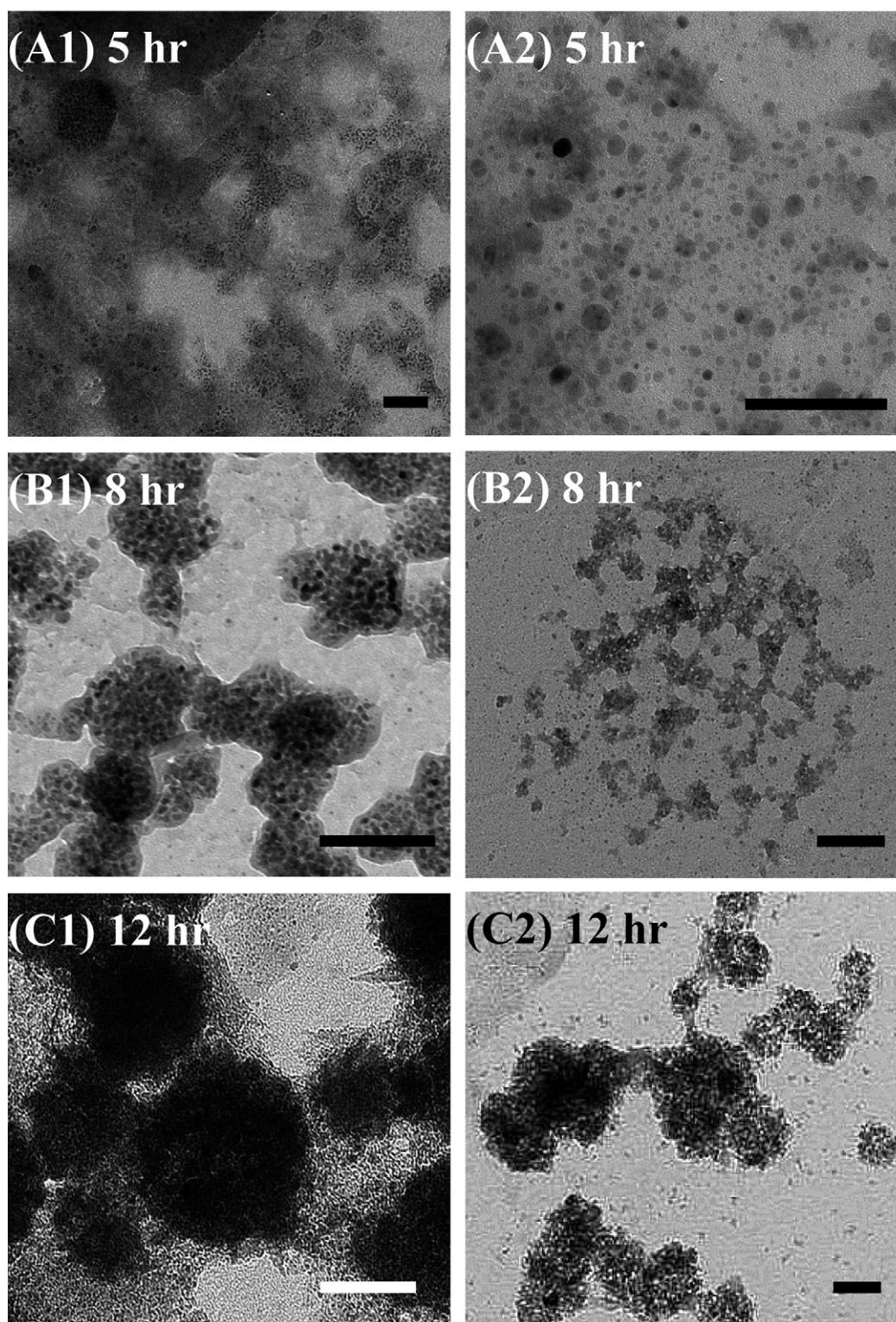


Fig. 9. (A–C) Control of microstructures of silica nanoparticles by changing the gellation time during salt-assisted aerosol synthesis. The temperature of tube furnace is 150 °C. The bar represents 100 nm.

take place so fast that the rapid precipitates of the salt resist the further structural collapse during the drying, otherwise the sols are stuck strongly each other. In this regard, aerosolization, i.e., misting the solution into droplets, supplies most fast drying process.

3.2.2. Role of salt in salt-assisted aerosol–gel synthesis of SiO_2 particles

As mentioned in the previous section, it is interesting to see whether or not the salt plays the same roles in salt-assisted aerosol–gel reaction. Fig. 9 shows the temporal evolution of sil-

ica particles before and after washing the salt. The overall trends of the structural changes are very similar to those in the batch reaction. Heating at relatively high temperature (150 °C) in the furnace forces the solvent to evaporate within the residence time (ca. 1 s). Compared to the 10 min in the batch reaction, this rapid drying allows the salt originally in liquid state to invade the open spaces inside a silica aggregate and then precipitates therein. As a filling agent of the open space, the nucleated fine salts reside the space, the composite structure of which will be preserved even at higher temperature but lower than the salt melting point. As the small spaces occupied by the salt are likely to be void pores after washing the salt, the resultant structure should be porous. Successfully, we confirmed this inference is quite true (see Fig. 9C1 and C2). The specific surface area (SSA) of such porous particles is measured by gas sorptometer (nitrogen adsorption at 77 K using Brunauer–Emmett–Teller (BET) analysis). The SSA of particles in Fig. 9C2 reaches ca. $335 \text{ m}^2 \text{ g}^{-1}$, accompanying the growth of pore volume up to $0.45 \text{ cm}^3 \text{ g}^{-1}$.

At the earlier t_g (5 h), isolation of silica sols by the salt is again observed as seen in Fig. 9A1 and A2. At the intermediate t_g (8 h), the microstructures in Fig. 9B1 and B2 seem to lie between the cases of the earlier and the longer times. Magnification of Fig. 9B1 revealed that the ultrafine silica sols are weakly connected each other and also embedded in a particle-like matrix. Washing the salt leads to partial breakage of the links and thereby leaving a fragmented structure like in Fig. 9B2. We would like to emphasize the microstructures controllable simply by altering the gelation time are ranged from isolated dots through fragments to mesoporous particles.

4. Conclusions

In this paper, we determined that there exists a common role of the inert salt in the two different aerosol-based syntheses of CuO and SiO₂ nanoparticles. The primary role of the salt added into the precursor solution is a filler to avoid agglomeration of nanoparticles. For the salt-assisted spray pyrolysis synthesis (SAS) of CuO particles, higher addition of the NaCl weakened the bonding of primary particles and removal of the salt led therefore to some fragmented structure. A little less dose of the salt in the SAS allowed to generate mesoporous CuO particles. Also, compared to the case of zero addition of salt, the existence

of the salt resulted in a significant morphology change from shell-like to solid-like structure. This was attributed to increase in the total salt content as well as homogeneous precipitation of the salt facilitated by the retarded evaporation. By using the salt-assisted aerosol–gel route, we could control the micro structure from a new nanometer dots through fragments to highly porous particles. In this case, the salt acts as not only a filler but also a catalyst for the reaction.

Acknowledgement

The authors gratefully acknowledge that this work was supported by Korea Research Foundation Grant funded by Korean Government (MOEHRD) (Project No. R08-2003-000-10858-0).

References

- [1] S.E. Pratsinis, *Prog. Energy Comb. Sci.* 24 (1998) 197.
- [2] D. Lee, S. Yang, M. Choi, *Appl. Phys. Lett.* 79 (2001) 2459–2461.
- [3] A. Prakash, A.V. McCormick, M.R. Zachariah, *Chem. Mater.* 16 (2004) 1466–1471.
- [4] K. Park, D. Lee, A. Rai, D. Mckherjee, M.R. Zachariah, *J. Phys. Chem. B* 109 (2005) 7290–7299.
- [5] R. Mahadevan, D. Lee, H. Sakurai, M.R. Zachariah, *J. Phys. Chem. A* 106 (2002) 11083–11092.
- [6] C.J. Brinker, G.W. Scherer, *Sol–Gel Science: The Physics and Chemistry of Sol–Gel Processing*, Academic Press, New York, 1989.
- [7] A. Martino, S.A. Yamanaka, J.S. Awola, D.A. Loy, *Chem. Mater.* 9 (1997) 423–429.
- [8] M.F. Skandar, K. Okuyama, F.G. Shi, *J. Appl. Phys.* 89 (2001) 6431–6434.
- [9] S.H. Kim, B.Y.H. Liu, M.R. Zachariah, *Langmuir* 20 (2004) 2523–2526.
- [10] K. Okuyama, I.W. Lenggoro, *Chem. Eng. Sci.* 58 (2003) 537–547.
- [11] J.H. Kim, V.I. Babushok, T.A. Germer, G.W. Mulholland, S.H. Ehrman, *J. Mater. Res.* 18 (2003) 1614–1622.
- [12] B. Xia, I.W. Lenggoro, K. Okuyama, *Chem. Mater.* 14 (2002) 2623–2627.
- [13] S.H. Kim, B.Y.H. Liu, M.R. Zachariah, *Chem. Mater.* 14 (2002) 2889–2899.
- [14] I.W. Lenggoro, T. Hata, F. Iskandar, M.M. Lunden, K. Okuyama, *J. Mater. Res.* 15 (2000) 733–743.
- [15] I.W. Lenggoro, K. Okuyama, J.F. Mora, N. Tohge, *J. Aerosol Sci.* 31 (2000) 121–136.
- [16] B. Xia, I.W. Lenggoro, K. Okuyama, *Adv. Mater.* 13 (2001) 1579–1582.
- [17] D. Lee, J.-W. Kim, B.G. Kim, *J. Phys. Chem. B* 110 (2006) 4323–4328.
- [18] J.Y. Kim, J.A. Rodriguez, J.C. Hanson, A.I. Frenkel, P.L. Lee, *J. Am. Chem. Soc.* 125 (2003) 10684–10692.